International Journal of Advanced and Applied Sciences

Journal homepage :http://www.ijaas.in

Properties of Vietnamese water caltrop starch and formation of low glycemic index starch

Khanh Son Trinh [1, *], Thuy Linh Nguyen [2], Thanh-Hoa Dang-Thi [2]

[1]*Faculty of Chemical and Food Technology, Ho Chi Minh City University of Technology and Education, Ho Chi Minh City, Vietnam*
[2]*Faculty of Fisheries, Nong Lam University, Ho Chi Minh City, Vietnam*

ARTICLE INFO

Article history:
Received 3 February 2023
Received in revised form
11 June 2023
Accepted 16 June 2023

Keywords:
Low glycemic index
Texture
Retrogradation
Water caltrop starch

ABSTRACT

This research investigates the properties and modification of water caltrop starch (WCS) with a particular focus on its potential for retrogradation and resistance to enzymatic hydrolysis. The study begins by obtaining WCS with a recovery efficiency of 4.5% (w/w in dry basis). The native WCS exhibits notable characteristics, including an apparent amylose content of 45.4%, a ratio of amorphous/α-helix regions at 1.341, a degree of relative crystallinity of 54.43%, an average molecular weight of 6.58×104 g/mole, and a degree of polymerization of 365.57. The high amylose content and degree of crystallinity in native WCS indicate its favorable retrogradation potential and resistance to enzymatic hydrolysis. Textural analysis of the WCS gel reveals high hardness and chewiness but low adhesiveness, which further supports its potential for retrogradation applications. To explore the effects of repeated retrogradation cycles, native WCS was subjected to 3, 6, and 9 cycles. The increase in retrogradation cycles led to a decrease in apparent amylose content from 31.79% to 29.34%. This reduction can be attributed to the formation of double helix associations and the emergence of new crystalline regions from amylose molecules. Furthermore, an increase in retrogradation cycles resulted in enhanced syneresis of starch. Interestingly, as the number of retrogradation cycles increased, the enzymatic hydrolysis rate of retrograded WCS gradually decreased. Correspondingly, the estimated glycemic index (GI) of the samples decreased, reaching a range of 50.05 to 38.46. Consequently, treatment with repeated retrogradation proves to be an effective strategy for producing modified WCS with a low glycemic index (<50%), thereby presenting promising opportunities for low glycemic index applications.

1. Introduction

Water caltrop (*Trapa bispinosa* Roxb.) is a plant with leaves floating on the surface of the water, with fruit and flowers. The fruit is shaped like a cow's head, with two curved horns. The horn-like spines are very sharp. Each fruit contains a large, starchy, and edible kernel. The seeds are eaten raw, boiled or roasted, and ground to create a powder used in cooking and medicine (Caballero et al., 2003). In India, this fruit can be eaten raw or cooked and they have become a popular street food here. Besides, this fruit can be made into porridge or mashed into chappatis. In China, this fruit can be boiled or grilled as a snack, and sold by vendors lining the streets. They can also be fried, candied, or powdered as a thickener or used to make bread, other baked goods, and candies. In Cambodia, Laos, and Vietnam, fruits are also roasted and eaten to reduce fever and relieve headaches (Wiart, 2013).

A previous study (Gao et al., 2014) compared starches obtained from three different Trapa species including *Trapa quadrispinosa*, *Trapa bispinosa,* and *Trapa pseudoinisa*. The results showed that the starch content (%) accounted for 6.61–16.6 of the dry kernel weight. The content (%) of amylose ranged from 27.69 to 30.23; the size of starch particles was from 13.97 to 17.47 μm; the solubility was from 18.7 to 20.0 g/g (at 95°C). Among them, *Trapa pseudoinisa* had the highest amylose content and particle size, and solubility/swelling.

Starch retrogradation is a process that occurs only in gelatinized starch. Amorphous regions are converted to more ordered or crystalline regions

resulting in changes in physicochemical properties (e.g., decrease in water-holding capacity), and rheological properties (e.g., increase in hardness, etc.). Retrogradation occurs only when the amount of water in the starch suspension is sufficient and the storage temperature is suitable (Eliasson, 2017). Retrogradation takes place strongly when the amylose-containing starch gel is stored at a cold temperature. Although amylopectin can also be retrograded, amylose molecules tend to recrystallize and form more hydrogen bonds. When retrograded, starch gel solution tends to increase turbidity and increase hardness (Eliasson, 2017).

The glycemic index (GI) is the index of the glycemic response of the specified amount of carbohydrate in a food with a corresponding amount of carbohydrate from the standard food consumed by the same subject (Jenkins et al., 2002). GI is divided into 3 levels: Low (≤55), moderate (56-69), and high (≥70) (Trinidad et al., 2013). Consuming high-GI foods will rapidly increase blood glucose levels thereby causing a series of hormonal and metabolic changes that promote excessive energy absorption into the body thereby causing obesity (Augustin et al., 2002; Jenkins et al., 2002). Meanwhile, a low GI diet in healthy people helps reduce the amount of C-peptide in the urine. In patients with diabetes or hyperlipidemia subjects, a low GI diet helps control blood glucose and reduce serum lipids. Low-GI diets help increase high-density lipoprotein cholesterol, reducing diabetes and cardiovascular disease risk. Many studies also show a reduced risk of colon and breast cancer in people using low-GI diets. It can be said that using a low-GI diet is important in preventing and treating many chronic diseases (Jenkins et al., 2002).

Theoretically, many factors can affect the digestibility and GI of starch. Factors such as amylose content, resistant starch, dietary fiber, etc… are correlated with low GI value. In addition, factors such as gelatinization or retrogradation can also alter the GI value of starch. RS_3 is a retrograded starch that has been shown to have a low GI value due to its low hydrolysis by digestive enzymes from which glucose is released (Lal et al., 2021).

In this study, we isolated and investigated some chemical, physicochemical and rheological properties of native WCS. Then, repeated cycles of retrogradation were used to produce modified WCSs with low GI.

2. Methods and materials

2.1. Retrogradation of water caltrop starch (WCS)

Water caltrop (*Trapa bispinosa* Roxb.) was harvested from Dong Thap province, Vietnam, within a period of 80 to 82 days from planting. After harvesting, the fruits were washed to remove dirt. After that, the fruits were soaked in 0.2% NaOH for 10-12 days (replacing the NaOH solution every day) to remove the color in the skin, thereby limiting the influence on the color of the starch obtained later. Soaking in NaOH also helps soften the peel of the fruit, thereby facilitating the separation of the starch inside the tuber. Then, the water caltrop pulp was milled and sieved (120 mesh) to form a suspension in 0.2% NaOH. The suspension was stirred, and allowed to settle. The NaOH solution was changed frequently until no traces of protein were detected (with the ninhydrin reagent). Then, the starch residue was soaked in distilled water (D.W) and adjusted to pH 7.0 with an HCl solution. The starch suspension in water was allowed to settle and continued to be washed with D.W. until no trace of NaCl remained (tested with $AgNO_3$). The starch residue was air-force dried at 50°C for 24 hours to reach a final moisture content of less than 12% (w/w). Starch was ground and sieved (120 mesh). The native water caltrop starch (WCS) was stored in vacuumed zip bags under dry conditions until used.

Retrograded starches were prepared through repeated cycles of retrogradation. First, the starch suspension (20%, w/v) was completely gelatinized in a sealed glass container (121°C, 30 min). Then, the starch paste was cooled to room temperature (30°C) (García-Alonso et al., 1999). For each cycle of retrogradation (24h), the starch gel was stored at 5°C/20h and subsequently stored at 30°C/4h (Muir and O'Dea, 1992).

Samples MA0, MA3, MA6, and MA9 corresponded to native starch and retrograded starches with 3, 6, and 9 cycles of retrogradation, respectively. At the end of each 3, 6, or cycles, the starch gel was spread thinly and dried at 50°C for 24 h to achieve a final moisture content of <12% (w/w). The MA sample was a completely gelatinized WCS (autoclaved at 121°C, 15 min) followed by drying. Modified starches above were ground and sieved (120 mesh). Starches were stored in vacuumed zip bags under dry conditions until used.

The recovery yield (H%) of starches preparation was calculated by the formula: $H(\%)=\frac{m_b}{m_o}\times 100\%$. Where m_b and m_o were the weight of the raw material and the weight of the obtained product.

2.2. Apparent amylose content (AM)

The amylose content was estimated by reacting starch with iodine. Apparent amylose content in starch was determined based on a published method (Zhu et al., 2008). Starch (100 mg) was placed in a 100 ml-volumetric flask. Ethanol (1.0 ml) was added to wet the sample. Next, 1N NaOH solution (10 ml) was added, gently shaken to dissolve the sample, and allowed to stand for about one hour until the solution was completely clear. Then make it up to 100 ml with D.W. This solution (2.0 ml) was removed and placed in another 100 ml-volumetric flask. Distilled water (50 ml) and 1% (w/v) phenolphthalein (2 drops) were added. 0.1N HCl solution was used to titrate the solution to neutral pH. Then, two ml of 0.2 % iodine solution (2.0 g KI

and 0.2 g I_2 diluted 100 ml with D.W) was added. D.W. was added to make a final volume of 100 ml. This final solution was left to stand for 30 min in the dark for coloration. The absorbance (Abs) of the sample was measured with a UV-Vis instrument (Halovis 20, Switzerland) in the wavelength range from 400 to 800 nm, at a distance of one nm. The amylose ratio was determined based on the absorbance of the solution by the formula: $AM(\%)=\frac{(Abs_{620}-Abs_{510})}{0.3995}$. Where, Abs_{620} and Abs_{510} were the absorbances of the sample at 620 nm and 510 nm, respectively.

2.3. Average molecular weight (Mw) of WCS

The average molecular weight of WCS was determined indirectly through kinematic viscosity (η, m^2/s), intrinsic viscosity (η_i, ml/g), relative viscosity (η_{rel}), and reduced viscosity (η_{rel}, ml/g) based on previous studies (Cowie, 1960; Harding, 1997; Dokic et al., 2004) and described in detail by previous authors (Trinh and Dang, 2019). An Oswald viscometer (∅=0.3 mm, Ref.No 509 03, Germany) was used to estimate the kinematic viscosity of a sample. Based on the Staudinger-Mark-Houwink equation, the average molecular weight of starch was estimated as $\eta_i=KM^{\alpha}$ (K=1.18×10-3; α=0.89).

2.4. Morphology of WCS granules

The morphology of starch granules was imaged by Scanning Electron Microscopy at an accelerating voltage of 15 kV.

2.5. X-ray diffraction pattern (XRD) and degree of crystallinity (DRC)

A powder X-ray diffractometer (Model D5005, Bruker, Karlsruhe, Germany) was used to analyze the X-ray diffraction pattern and degree of relative crystallinity of starch samples. Cu-K radiation of 0.15406 nm (Nickel filter; time constant, 4 s) was used under 40 kV and 40 mA working conditions. Each scan was performed from 5 to 30° (2θ). The DRC was calculated using the equation: $DRC=\frac{A_c}{(A_c+A_a)}$, where A_c was the area of the crystalline portion and A_a was the area of the amorphous portion (Nara and Komiya, 1983; Gomes et al., 2010) with peak-fitting software (Origin version 8.5.1, Origin Lab, Northampton, Mass., U.S.A.).

2.6. Fourier transform infrared spectroscopy (FTIR) measurement

FTIR spectra were recorded following the method of a published paper (Kizil et al., 2002) at the wavenumber from 400 to 4400 cm^{-1}(FTIR-8400S, Shimadzu, Japan). Two grams of starch and 0.2 g of KBr were mixed well and pressed at 8.0 bar for 10 min before measurement

2.7. Swelling power (SP) and solubility index (SI)

The swelling power and solubility index were estimated using a method of a published paper (Kusumayanti et al., 2015; Leach et al., 1959). Starch (m_o, 2.0 g) and D.W (10 ml) were added to a centrifuge tube and mixed carefully. The starch suspension was kept at 95°C for 30 min with continuous shaking. Then, the starch paste was cooled to room temperature and then centrifuged at 1000 ×g for 20 min. The centrifugal residue was weight (m_1, g). The supernatant was dried at 105°C for 24 h and weight (m_2, g). The swelling power was calculated as $SP(g/g)=\frac{m_1}{(m_o-m_2)}$. The solubility index was calculated as $SI(\%)=\frac{m_2}{m_o}\times100\%$.

2.8. Freeze-thaw stability (syneresis) of starch

Freeze-thaw stability of starches was calculated mainly based on a published method (Wang et al., 2016) with slight modifications. The starch suspension (30 ml, 6%, w/v), in a 50 ml-centrifuge tube, was completely gelatinized at 95°C for 30 with continuous shaking. Then, the starch paste (m_o) was cooled to room temperature (30°C). For one cycle of freeze-thaw, the representative starch paste was kept in a freezer (-18°C, 24h). Next, the starch paste was placed in a water bath (30°C, 1.5h) for thawing and equilibration. At the end of each cycle, the starch paste was kept in a freezer for the next cycle or was centrifuged (1000 ×g, 15 min). The supernatant was decanted completely and the centrifuged sediment was weighted (m_1). The syneresis (%)=weight (g) of centrifuge sediment/weight (g) of starch paste ×100%.

2.9. Texture profile analysis of WCS

Texture profiles are important indicators in evaluating product quality, especially starch gel products. TPA (texture profile analysis) is a popular dual compression test to determine the textural properties of food materials (Nassar et al., 2017). The native WCS slurry (15, 20, and 25 %, w/v in dry basis) was fully gelatinized (95°C, 15 min), then fixed in a mold and allowed to cool to room temperature to form a cylindrical gel (height of 19 mm, a diameter of 44 mm). The gel was wrapped in polyethylene film and allowed to stabilize for 1h before measurement. TPA was performed only with gel samples (>15%, w/v) which were able to retain their shape after removal from the mold.

TPA was measured using a CT3 Texture Analyzer (Brookfield Ametek, USA). The compression test was done using a 4500 g load cell. The parameters of analysis were: Target value of 5.0 mm, trigger load of 5.0 g, test speed of 1.0 mm/s, return speed of 1.0 mm/s, the distance between sample and probe was 10.0 mm, TA-AACC36 probe, TA- RT-KIT fixture. TPA parameters were calculated based on a previous study (Nassar et al., 2017).

2.10. Hydrolysis rate and estimated glycemic index (Est. GI) of starches

Starch (5.0 g, w/v) was suspended with phosphate buffer solution (50 ml, pH 5.8) in a 100 ml-shake flask with a magnetic stirrer and kept at 37°C for 30 min. Diluted α-amylase (12 U/ml, Termamyl LS 120, Novozyme, Denmark) was kept at 37°C until use. Then, an enzyme solution (0.5 ml) was added to the starch suspension. The reaction was conducted for 420 min. At various intervals of hydrolysis time, the sample (1.0 ml) and DNS reagent (4 ml) were put into a 15 ml-centrifugal tube, mixed well, boiled for 10 min, and then cooled to room temperature. This solution was centrifuged (3500 ×g, 10 min). The absorbance (λ_{540nm}) was measured using a UV-Vis spectrophotometer. Reducing sugar in a sample was a quantitative analysis by the DNS method (Miller, 1959). A blank sample was prepared as the above description using D.W. instead of the enzyme. A linear standard curve (R^2 >0.95) was done using maltose for calculation.

All enzymatic hydrolysis curves were fitted to Goni's equation (Arp et al., 2020; Goñi et al., 1997) using the Solver in Excel software (version 2019, Microsoft Corporation, USA): $C=C_\infty(1\text{-}e^{-kt})$, where C, C_∞, k, t were reducing sugar content, the maximal value of reducing sugar (at $t \to \infty$), constant rate, and hydrolysis time, respectively. The area under curves (AUC) of samples from the above fitting curves was estimated by Origin software (version 8.5.1, Origin Lab.). AUC of amorphous water caltrop starch (MA, 5% w/v, autoclaved at 121°C, 15 min) was used as the reference sample.

2.11. Statistical analysis

All values were shown in the mean (±SD) (n=3). The data were calculated differently by one-dimensional ANOVA calculation (p<0.05, Duncan's multiple range test) using SPSS software (released 2008, SPSS Statistics for Windows, version 17.0, Chicago: SPSS Inc.).

3. Results and discussion

3.1. Composition of water caltrop tuber and yield of water caltrop starch extraction

The moisture content of the entire tuber was found to be 79.92% (w/w), while the moisture content of the peel and kernel was determined to be 80.07% and 79.76%, respectively. Additionally, the relative proportions of peel and kernel, calculated on a dry weight basis, were 50.35% and 49.65%, respectively. The efficiency of starch recovery was measured at 4.5% (w/w) on a dry weight basis.

3.2. Viscosity and average molecular weight of WCS

Dissolved in a 1.0 M KOH solution, intrinsic viscosity (η_i, ml/g) was affected by the structure, size, shape, and molecular weight (M_w) of starch molecules (Cui, 2005). Thus, Mw of starch could be estimated (at 30°C) by intrinsic viscosity (Harding, 1997; Dokic et al., 2004). M_w of WCS was 6.58×10^4 g/mole, and the average degree of polymerization (DP) was 365.57 (Table 1). Besides, Fig. 1 showed that MA0 was completely soluble in 1M KOH solution. Meanwhile, samples MA3, MA6, and MA9, after being mixed with 1M KOH and left to stand, were quickly separated into the sediment below the KOH solution. This showed that these samples are difficult to dissolve due to strong retrogradation (more hydrogen formation).

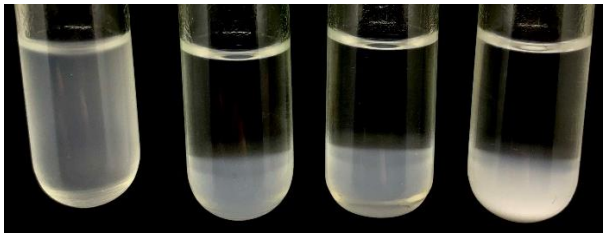

MA0 MA3 MA6 MA9

Fig. 1: Solution of starch samples in 1M KOH

Table 1: Parameters of starches

Properties	Samples			
	MA0	MA3	MA6	MA9
Apparent amylose content (%)	45.40±0.08^c	31.79±0.18^b	29.67±1.85^{ab}	29.43±0.61^{ab}
Recovery yield (%)	-	99.09±0.02^a	98.28±0.01^b	97.81±0.01^c
The ratio of amorphous/α-helix regions (A/H)	1.341±0.01^d	1.028±0.01^a	1.037±0.00^b	1.042±0.00^c
Degree of relative crystallinity (DRC,%)	54.43±0.55^d	43.82±0.41^a	46.47±0.39^b	49.19±0.17^c
Swelling power (SP)	11.24±0.05^a	11.53±0.69^{ab}	11.91±0.57^{ab}	13.16±0.33^d
Solubility index (SI)	15.53±0.64^c	5.73±0.19^b	5.12±0.06^{ab}	4.82±0.03^a
Regression equation of reduced viscosity (η_{red}, ml/g) vs starch concentration (c, mg/l) at 30°C	$\eta_{red} = 70.95c + 22.92$ (R^2=0.9652)			
Average molecular (M_w, ×10^4 g/mol)	6.58			
Degree of polymerization (DP)	365.57			

The values in the table represented the mean (± standard deviation). Values with different symbols in the same row indicated a statistically significant difference (p< 0.05). DP = Mw of starch/Mw of glucose (180 g/mole)

3.3. Texture profile of WCS gel

The texture properties of WCS gels were shown in Fig. 2 and Table 2. Hardness is defined as "the peak force during the first compression cycle" or "the force needed to attain a given deformation" (Pons and Fiszman, 1996). The results showed that hardness increased gradually with increasing starch concentration (15-25%, w/v). The starch gel with high hardness typically has a high amylose content and/or a long amylopectin chain. Besides, gel hardness is mainly due to starch retrogradation (which begins to happen during the cooling step of gel formation), related to water syneresis and amylopectin recrystallization (Eliasson, 2017). There were not many differences between 1st peak force and 2nd peak force indicating WCS gels had good state recovery ability after the first compression. Hardness was directly proportional to the starch content in the WCS gel. Furthermore, there was little difference between 1st peak force and 2nd peak force, which showed that WCS gel has a good state recovery ability after the first compression (Fig. 2).

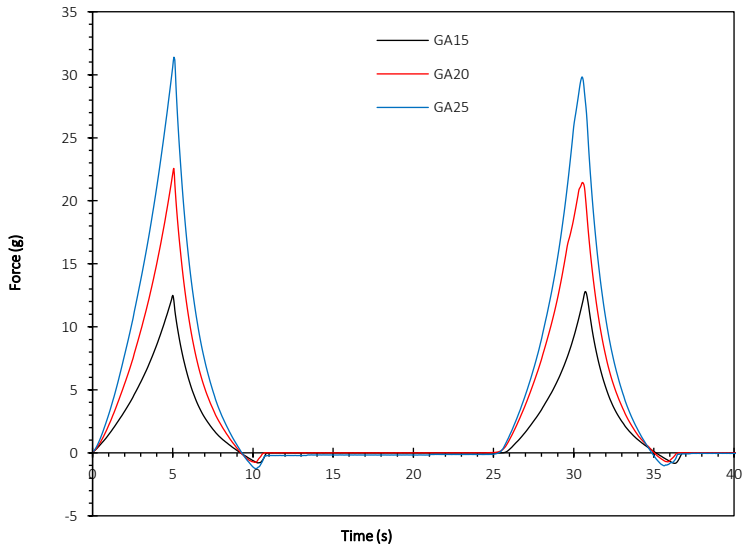

Fig. 2: Texture profile analysis (TPA) of WCS gel; (GA15, GA20, and GA20: WCS gel at concentrations of 15, 20, and 25% w/v)

Adhesiveness is defined as "the negative force area for the first bite, representing the work necessary to pull the plunger away from the food sample" or "the work necessary to overcome the attractive forces between the surface of the food and the surface of other materials with which the food comes in contact (e.g., tongue, teeth, palate, etc.). In other words, "adhesiveness is related to surface properties" (Pons and Fiszman, 1996). The adhesiveness of WCS gel increased proportionally with starch concentration. In general, WCS gel had low adhesion. Adhesiveness was affected by the structure of starch. A decrease in amylose molecular weight or a decrease in the number of branched chains of amylopectin molecules increased adhesiveness (Pycia et al., 2015).

The chewiness is the amount of time it takes to chew a sample until it can be swallowed (Abdelghafor et al., 2011). In this study, chewiness increased proportionally with the concentration of WCS gel. Springiness is the ratio of time (or distance) of the second compression to that of the first compression (Pons and Fiszman, 1996). Resilience is the ability to restore the original position of the sample (Abdelghafor et al., 2011). Cohesiveness is the level of 2nd deformation compared to the 1st one (Abdelghafor et al., 2011). Table 2 showed that the springiness, resilience, and cohesiveness of the WCS gel samples have almost no difference from each other. The texture profiles of retrograded starches were not shown because these samples could not be completely gelatinized (at 95°C, 15 min) to form gels.

Table 2: Textural profiles of native WCS

Sample	Hardness (g)	Adhesiveness (g.s)	Springiness (ratio)	Resilience (ratio)	Cohesiveness (ratio)	Chewiness (g)
GA15	12.50±0.29^{c}	0.02±0.00^{a}	1.01±0.05^{a}	0.59±0.03^{a}	1.00±0.01^{a}	12.63±0.86^{b}
GA20	22.54±0.88^{e}	0.03±0.01^{ab}	0.97±0.05^{a}	0.62±0.04^{a}	1.05±0.04^{a}	22.72±0.84^{d}
GA25	31.39±0.51^{f}	0.10±0.01^{c}	0.96±0.04^{a}	0.63±0.05^{a}	0.94±0.00^{a}	28.47±1.19^{e}

The values in the table represented the mean (± standard deviation). Values with different symbols in the same column indicated a statistically significant difference ($p< 0.05$). GA15, GA20, and GA25 were the gel of native water caltrop starch at 25, 20, and 30% (w/v)

3.4. Amylose content

The color of the starch-iodine complex changed from violet-blue (DP 39-40) to brown (DP 21-24). If DP<20, linear molecules could not bind to iodine (Cui, 2005). Starch molecules with DP 14-38, DP 45, and DP 400 have maximum absorbance at wavelengths 490-555, 568, and 645 nm, respectively (Eliasson, 2017; Cui, 2005). In this study (Fig. 3), native starch had Abs_{max} at λ=606 nm. Meanwhile, retrograded starches had Abs_{max} at λ=583-594 nm. In addition, when increasing the number of

retrogradation cycles, the absorbance intensity of the starch sample was gradually reduced in the order: MA0<MA3<MA6≈MA9. Thus, among the samples, the amylose content of native WCS was the highest (45.40 %). As the retrogradation cycle increased from 3 to 9 cycles, the amylose content gradually decreased from 31.79 to 29.43% (Table 1). The amylose content could be determined colorimetrically from the starch-iodine complexation. In the amorphous region, the conformation of amylose molecules was in a single helical state or random coil. Dispersed amylose on retrogradation could form double helix associations (DP 40-70), which cannot bind to iodine for complexion (Jane and Robyt, 1984). In other words, a small amount of amylose of retrograded starches was reassociated and quickly separated into the sediment below the NaOH solution. As a result, during retrogradation, the amount of blue complex of starch-iodine was gradually reduced. This explained why the blue complex is often used to monitor the starch retrogradation process (Wang et al., 2015).

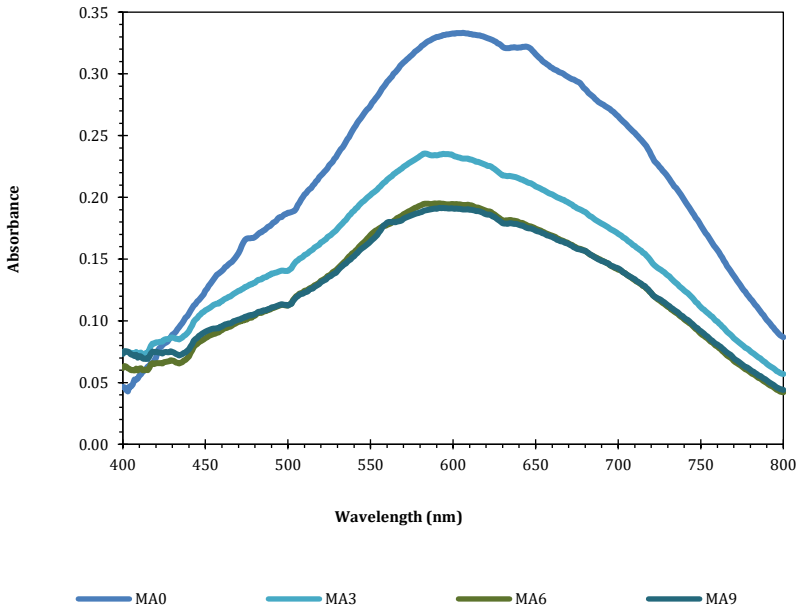

Fig. 3: Wave-scanning of starch-iodine complexes

3.5. Changes in chemically functional groups of starch

FTIR spectroscopy is an analytical measurement used to evaluate and relatively characterize chemical changes in starch. FTIR is also used for the determination of process-induced changes and the quality of foods (Eliasson, 2017). According to a previous report (Kizil et al., 2002), FTIR spectra of a starch sample could be divided into 4 parts (Fig. 4): (a) the region below <800 cm^{-1}, (b) the fingerprint region (800-1500 cm^{-1}), (c) C-H stretch region (2800-3000 cm^{-1}) và (d) O-H stretch region (3000-3600 cm^{-1}). In this study, bands at 533 and 578 cm^{-1} were attributed to the skeletal modes of the pyranose rings in starch. Highly overlapping and complex spectra were found in the region between 800-1500 cm^{-1}. The band at 930 cm^{-1} was attributed to the α-1,4 glycosidic linkages. The bands at 1094, 1169, and 1242 could be attributed to C-O-H bending modes, the coupling modes of C-O and C-C stretching, and the CH_2OH-related mode as well as the C-O-H deformation mode, respectively. Broadband with a peak at 1667 cm^{-1} was identified as the amorphous region of starches. So, the absorbance intensity of this band became lower indicating the increase in crystal regions in the sample. The C-H stretching modes were observed in the region of 2800-3000 cm^{-1}. The higher intensity of peak at this region indicated the higher content of amylose content in the sample. This was completely consistent with AM measurement results (Table 1). A very broadband at 3000-3600 cm^{-1} features an O-H stretching mode of starch.Starch is a semi-crystalline structure that includes amorphous and α-helix structural regions. A previous study (Capron et al., 2007) reported FTIR bands around 1022 and 1047 cm^{-1} that were attributed to amorphous and α-helical regions in starch. The corresponding peaks in our study were slightly shifted towards higher wavenumber, 1027 and 1057 cm^{-1}, respectively (Fig. 4). It could be seen that the ratio of ordered (α-helix)/amorphous increases with an increasing number of retrogradation cycles. Even so, all retrograded starches had a lower percentage of this than that of the native starch. This was due to the difference in nature between the native sample (granular state) and the retrograded samples (non-granular state). In other words, firstly, the native sample was completely gelatinized (amorphous state). Then, progressive retrogradation took place (from MA3 to MA9) leading to a gradual decrease in the amorphous region and a gradual increase in the α-helix region.

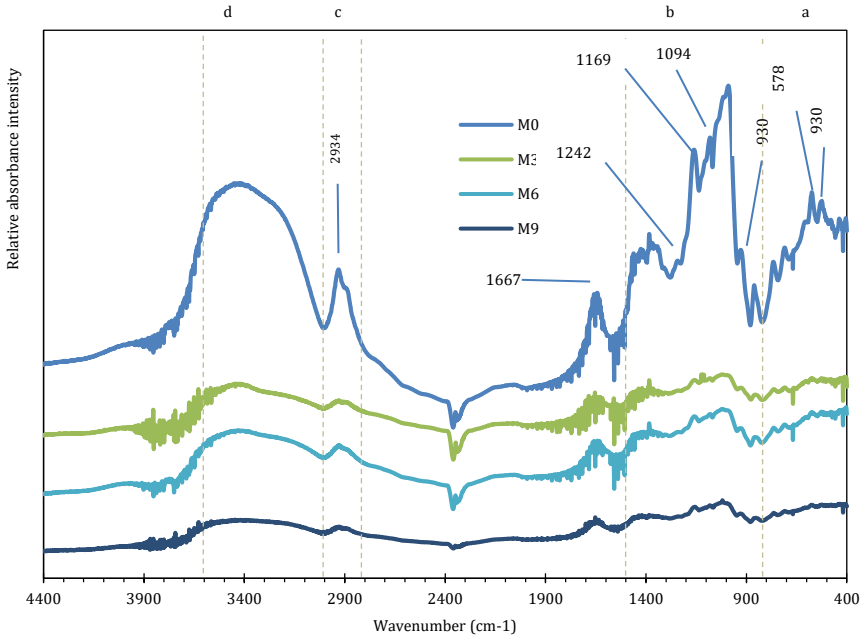

Fig. 4: FTIR spectra of starches

3.6. X-ray diffraction pattern of starches

X-ray diffraction patterns of starches were shown in Fig. 5. Native WCS had typical peaks for the A-type XRD pattern at 15.2°, 17.2°, 18.0°, 20.0° và 23.0° (2θ) (Eliasson, 2017). A previous study (Liu et al., 2021) reported water caltrop starch (*Trapa Taiwanensis* Nakai) with a C_A-type XRD pattern. Additionally, a previous study reported starch from *Trapa acornis* Nakano and *Trapa quadrispinosa* Roxb displayed an A-type XRD pattern whilst starch from *Trapa bicornis* Osbeck displayed a C_A-type XRD pattern (Feng et al., 2010). After being gelatinized (amorphous starch, XRD not shown), the reassociation (retrogradation) took place in this starch. As a result, re-crystallinity made DRC gradually increase corresponding to the number of retrogradation cycles (Table 1). The gelatinization-retrogradation process changed the XRD pattern of starches the intensities of the 15.2° and 12.7° (2θ) peaks in the MA3, MA6, and MA9 samples were lower than that of MA0. Shoulder peak at 18.0° in sample M0 absented from the XRD of retrograded starches. The peak at 20.0° in sample MA0 became wider and more intense in treated starches. The peak intensity of 20.0° (2θ) increased gradually with the retrogradation cycle. The peak at 23.0° in sample M0 was split into two new peaks of 22.3° and 24° in retrograded starches. Finally, a new peak, 29.5°, appeared in the treated starches and increased in intensity corresponding to the retrogradation cycle.

The degree of relative crystallinity (DRC) of starch samples was presented in Table 1. DRC of native starch was 54.43%. Previous authors (Liu et al., 2021; Feng et al., 2010) reported starch from *Trapa acornis* Nakano, *Trapa quadrispinosa* Roxb, *Trapa bicornis* Osbeck, and *Trapa Taiwanensis* Nakai had DRC of 39, 28, 40, and 38.98%, respectively. Thus, species, as well as a growing area, influence the crystal type and DRC of native WCS.

3.7. Swelling power (SP) and solubility index (SI)

Practically, starch could not be dissolved in excess water at temperatures lower than its gelatinization temperature (normally less than 60-70°C) due to the presence of semi-crystalline regions and H-bonds formed between the -OH groups. At a temperature higher than the gelatinization temperature, these bonds were broken and the free -OH groups will bind with water molecules causing swelling then the starch granule could be easily dissolved, and the starch paste will become clearer (Eliasson, 2017).

Swelling power indicates the water-holding capacity of starch (Kusumayanti et al., 2015). Table 1 showed the swelling power (SP, g/g) of the starch samples. Native WCS had a much lower SP (11.24) than waxy maize (28.5), and potato starches (39.2). However, native WCS had higher SP than sweet potato (>10) and high-amylose maize starches (6.56 or 7.1) (Singh et al., 2010; Virna Muhardina et al., 2016). The retrogradation process increased the SP of the starch sample, especially in the MA9 sample. In this study, the SP value was inversely Kusumayant proportional to the AM content of the samples. A previous study (Sasaki and Matsuki, 1998) stated there was an inverse correlation between swelling power and amylose content. In other words, amylose inhibited swelling. Amylopectin was the molecule that increases swelling and the amylose molecule acts as a diluent. However, SP was not only affected by the amylose content but also by the degree of starch crystallinity. The higher the crystallinity of the starch sample was, the more swelling inhibited was (Chaiyakul et al., 2016).

The solubility index (SI) was the amount of starch leached out into the supernatant during swelling power determination at a specified temperature (Kusumayanti et al., 2015). In this study, SI gradually decreased with the increasing retrogradation cycle (Table 1). Internal rearrangement of starch caused the increase of DRC or crystallite perfection leading to a decrease in starch solubility (Chaiyakul et al., 2016).

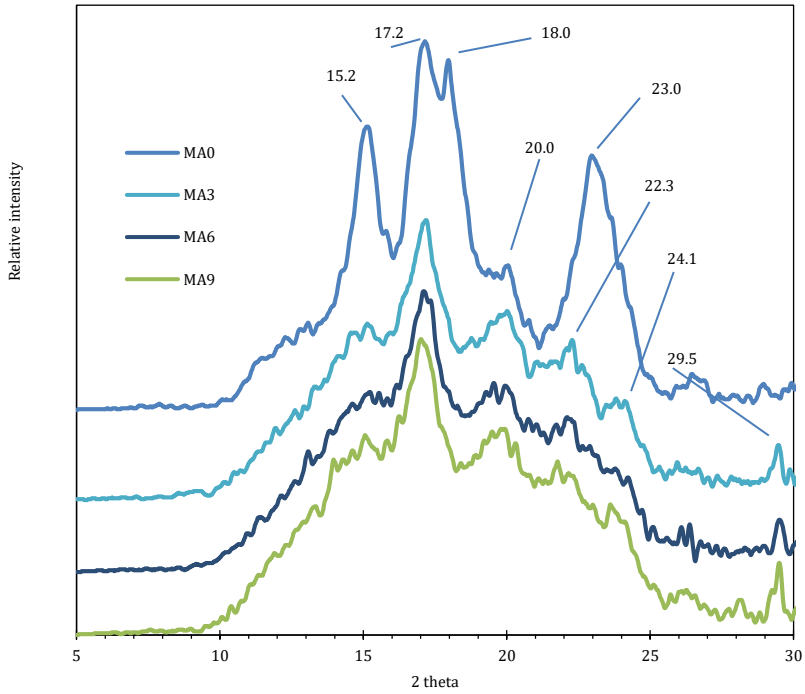

Fig. 5: X-ray diffraction patterns of starches

3.8. Freeze-thaw stability of starch

Freeze-thaw stability of starch was shown in Fig. 6. Retrogradation is a process that occurs in gelatinized starch, from initially an amorphous state to a more ordered or crystalline state. The result is an increase in firmness or hardness. During retrogradation, the water-holding capacity gradually decreases, and the crystallinity increases. Retrogradation takes place when storing starch gel with 40-50% water content at low temperature (but higher than glass transition temperature, T_g=-5.0°C). The retrogradation rate, when storing starch at low temperature, is faster than it is at room temperature. However, crystallites formed at low temperatures (4-5°C) will be less nearly perfect than crystallites formed at higher temperatures (Eliasson, 2017). The results of this study showed that the syneresis increases with the number of freeze-thaw cycles. In addition, the syneresis increased with the number of cycles of retrogradation. In other words, the increase in the freeze-thaw cycle led to an increase in retrogradation and the syneresis of the samples (Fig. 6).

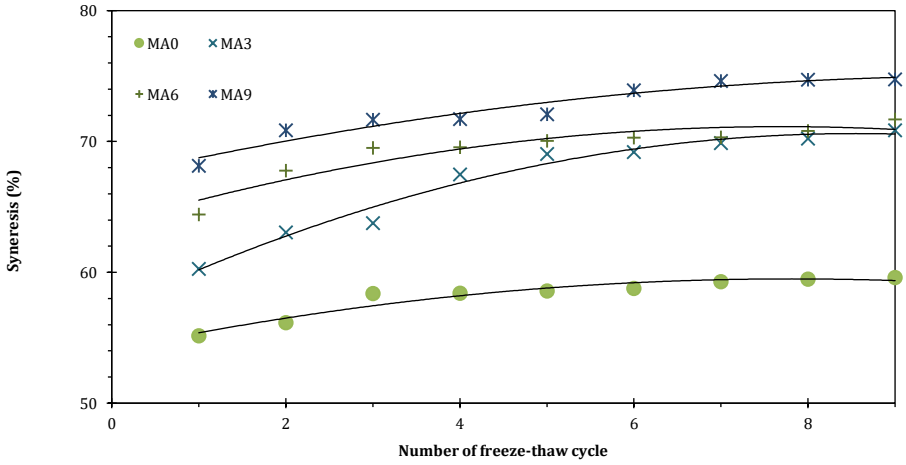

Fig. 6: The syneresis of starches

3.9. Degree of starch hydrolysis and estimated glycemic index

Under attacks of amylase on the granules of various sources of starches, five patterns have been observed and described: Pinhole, sponge-like erosion, several medium-sized holes, single hole (Fig. 7), and surface erosion (Evers, 1979). Fig. 7 showed that the granules of the native sample had a smooth surface and were free from cracks, fissures, or spores; meanwhile, the hydrolyzed granule was corroded to form a large hole through which the hydrolytic agents penetrate the granules (Trinh and Dang, 2019).

According to Fig. 7, the hydrolysis rate increases with reaction time. In other words, the higher the maltose content was, the greater the degree of hydrolysis of the sample was. The degree of hydrolysis of the samples over 0-420 min was ranked in the following order: MA0<MA9<MA6<MA3<MA. In these samples, MA0 was the sample in the granular state. Meanwhile, the remaining samples were in a non-granular state. Gelatinization has transformed crystalline regions into amorphous regions, which are easily attacked by alpha-amylase. Besides, retrogradation increased DRC, thereby limiting enzyme attacks on starch (Arp et al., 2020; Eliasson, 2017).

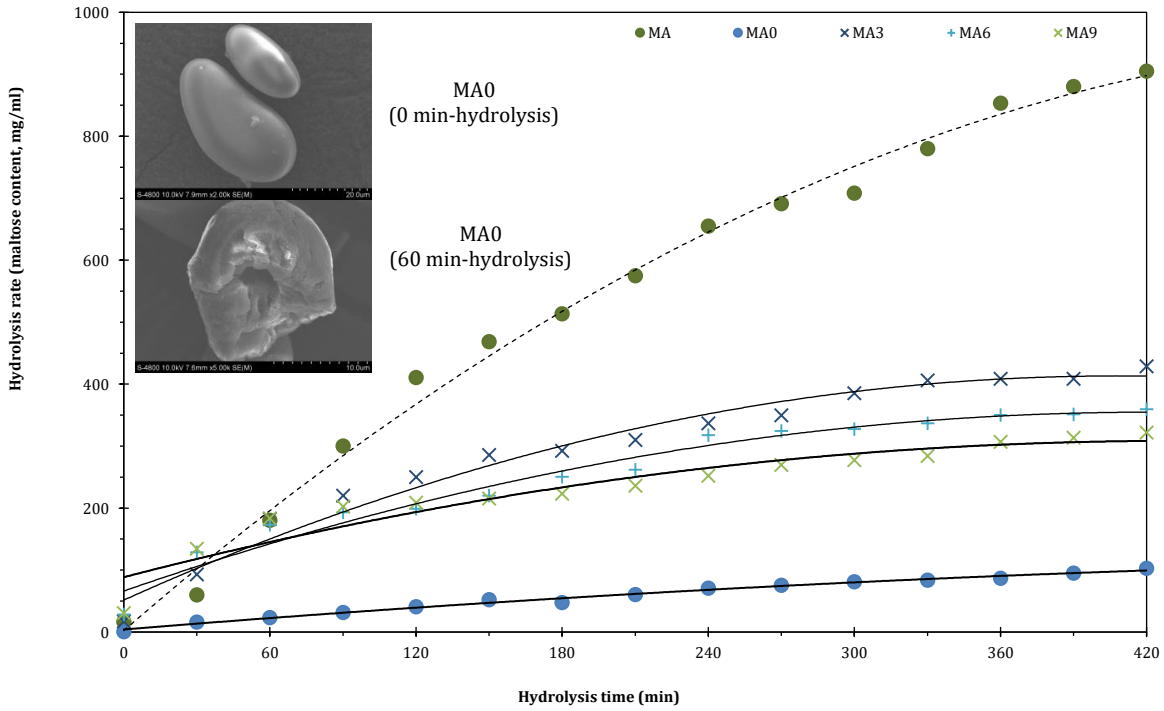

Fig. 7: Curves of α-amylase hydrolysis of starches

The results showed that the native starch was difficult to hydrolyze because it was still in a granular state and its crystallinity was highest (53.433%). For gelatinized and retrograded samples, it could be seen that gelatinized sample was hydrolyzed more and faster than retrograded ones. Gelatinized starch lost its ordered structure, so the enzyme can easily attack the amorphous regions (Botham et al., 1994; Eliasson, 2017). Compared with the amorphous sample (MA), retrograded starch samples (MA3-MA9) had a high degree of crystallinity, so they were less susceptible to enzymatic hydrolysis. Sample MA3 was hydrolyzed faster than samples MA3 and MA9. The hydrolysis rate of non-granular state samples was ranked in the following order: MA9<MA6<MA3<MA (Fig. 7). This order was also proportional to their degree of crystallinity (DRC). As the freeze-thaw cycle increased, the degree of starch retrogradation became higher, forming more crystalline regions and making the starch sample difficult to hydrolyze by alpha-amylase.

Table 3 shows that C_∞ (the maximal value of reducing sugar) and the estimated glycemic index of water caltrop starches were arranged in the following order: MA>MA3>MA6>MA9>MA0. Especially, all three samples MA3, MA6, and MA9 were low GI starch (Trinidad et al., 2013). Thus, the retrogradation process significantly and extremely reduced the hydrolysis rate as well as the estimated glycemic index (Est. GI) of modified WCS. Comparing with the results from Tables 1 and 3, there was agreement in the results of the ratio of amorphous/α-helix regions (A/H), degree of relative crystallinity (DRC), and Est. GI. Retrogradation increased the proportion of structural regions, and crystallinity, and forms a more compact structure leading to a decrease in the digestibility of starch (Arp et al., 2020). Furthermore, in our study, retrogradation probably led to the formation of type 3 resistant starch by a new crystalline arrangement and formation (Eliasson, 2017; Jiang et al., 2020).

Table 3: Kinetic parameters of alpha-amylase hydrolysis curves and estimated glycemic index or native and retrograded starches

Sample	C_∞ (mg.ml^{-1})	k (min^{-1})	Adj. r^2	F test	Est. GI
MA	130.7809	0.0028	0.9770	e	100.00
MA0	14.1599	0.0028	0.9628	a	10.86
MA3	43.9721	0.0072	0.9709	d	50.05
MA6	38.8202	0.0061	0.9818	c	41.26
MA9	36.8219	0.0048	0.9551	b	38.46

The values in the table represented the mean. Values with different symbols in the same column indicated a statistically significant difference ($p< 0.05$)

4. Conclusion

Water caltrop starch, native to Vietnam, represents a relatively understudied type of starch, particularly concerning its physicochemical properties and texture. This study aimed to investigate these characteristics in detail. The findings revealed that native WCS exhibited elevated levels of amylose content and crystallinity. Notably, the WCS gel demonstrated high hardness but exhibited minimal adhesiveness and resilience. The considerable amylose content and hardness of WCS indicated substantial potential for retrogradation. However, direct consumption of native WCS was found to be impractical due to its limited digestibility. Nevertheless, the study demonstrated that a cycling retrogradation procedure could harness the potential of WCS to produce starch with a low glycemic index. Through nine cycles of retrogradation, the glycemic index of the resulting starches underwent a progressive reduction, eventually reaching a low level of 38.46. One of the significant advantages of this approach lies in its simplicity, making it amenable to large-scale implementation in industrial settings. Consequently, these findings open up promising avenues for utilizing water caltrop starch as an effective means of producing low glycemic index starches, further contributing to the diversification of starch-based applications.

Acknowledgment

We appreciate the cooperation of Ms. Xuan-Dung Pham-Thi (Student ID 15116075) and Ms. Thuy-Linh Tran-Thi (student ID 15116102). These students have supported us with enthusiasm and responsibility thereby helping to keep the research on schedule. We are also grateful to Ho Chi Minh University of Technology and Education for providing the facilities for us to carry out this study.

Compliance with ethical standards

Conflict of interest

The author(s) declared no potential conflicts of interest with respect to the research, authorship, and/or publication of this article.

References

Abdelghafor RF, Mustafa AI, Ibrahim AMH, and Krishnan PG (2011). Quality of bread from composite flour of sorghum and hard white winter wheat. Advance Journal of Food Science and Technology, 3(1): 9-15.

Arp CG, Correa MJ, and Ferrero C (2020). Production and characterization of type III resistant starch from native wheat starch using thermal and enzymatic modifications. Food and Bioprocess Technology, 13: 1181-1192. https://doi.org/10.1007/s11947-020-02470-5

Augustin LS, Franceschi S, Jenkins DJA, Kendall CWC, and La Vecchia C (2002). Glycemic index in chronic disease: A review. European Journal of Clinical Nutrition, 56(11): 1049-1071. https://doi.org/10.1038/sj.ejcn.1601454 **PMid:12428171**

Botham RL, Morris VJ, Noel TR, Ring SG, Englyst HN, and Cummings JH (1994). A comparison of the in vitro and in vivo digestibilities of retrograded starch. Gums and Stabilisers for the Food Industry, 7: 187-195.

Caballero B, Trugo L, and Finglas P (2003). Encyclopedia of food sciences and nutrition: Volumes 1-10. 2nd Edition, Elsevier Science, Amsterdam, Netherlands.

Capron I, Robert P, Colonna P, Brogly M, and Planchot V (2007). Starch in rubbery and glassy states by FTIR spectroscopy. Carbohydrate Polymers, 68(2): 249-259. https://doi.org/10.1016/j.carbpol.2006.12.015

Chaiyakul S, Sukkasem D, and Natthapanpaisith P (2016). Effect of flour concentration and retrogradation treatment on physical properties of instant sinlek brown rice. International Journal of Nutrition and Food Engineering, 10(12): 814-822.

Cowie JMG (1960). Studies on amylose and its derivatives; Part I: Molecular size and configuration of amylose molecules in various solvents. Die Makromolekulare Chemie: Macromolecular Chemistry and Physics, 42(1): 230-247. https://doi.org/10.1002/macp.1960.020420123

Cui SW (2005). Food carbohydrates: Chemistry, physical properties, and applications. 1st Edition, CRC Press, Boca Raton, USA. https://doi.org/10.1201/9780203485286

Dokic L, Jakovljevic J, and Dokic P (2004). Relation between viscous characteristics and dextrose equivalent of maltodextrins. Starch-Stärke, 56(11): 520-525. https://doi.org/10.1002/star.200400294

Eliasson AC (2017). Carbohydrates in food. 3rd Edition, CRC Press, Boca Raton, USA. https://doi.org/10.1201/9781315372822

Evers AD (1979). Cereal starches and proteins. In: Vaughan JG (Ed.), Food microscopy: 139-191. Academic Press, London, UK.

Feng Y, Nan G, and Guo-Hua Z (2010). Granular properties of water caltrop starch from three varieties. Food Science, (3): 118-122.

Gao H, Cai J, Han W, Huai H, Chen Y, and Wei C (2014). Comparison of starches isolated from three different Trapa species. Food Hydrocolloids, 37: 174-181. https://doi.org/10.1016/j.foodhyd.2013.11.001

García-Alonso A, Jiménez-Escrig A, Martín-Carrón N, Bravo L, and Saura-Calixto F (1999). Assessment of some parameters involved in the gelatinization and retrogration of starch. Food Chemistry, 66(2): 181-187. https://doi.org/10.1016/S0308-8146(98)00261-1

Gomes AMM, DA SILVA CEM, Da Silva PL, Ricardo NMPS, and Gallao MI (2010). Annealing of unfermented (polvilho doce) and fermented (polvilho azedo) cassava starches. Boletim do

Centro de Pesquisa de Processamento de Alimentos, 28(2): 223-232. https://doi.org/10.5380/cep.v28i2.20405

Goñi I, Garcia-Alonso A, and Saura-Calixto F (1997). A starch hydrolysis procedure to estimate glycemic index. Nutrition Research, 17(3): 427-437. https://doi.org/10.1016/S0271-5317(97)00010-9

Harding SE (1997). The intrinsic viscosity of biological macromolecules: Progress in measurement, interpretation and application to structure in dilute solution. Progress in Biophysics and Molecular Biology, 68(2): 207-262. https://doi.org/10.1016/S0079-6107(97)00027-8 **PMid:9652172**

Jane JL and Robyt JF (1984). Structure studies of amylose-V complexes and retro-graded amylose by action of alpha amylases, and a new method for preparing amylodextrins. Carbohydrate Research, 132(1): 105-118. https://doi.org/10.1016/0008-6215(84)85068-5 **PMid:6435871**

Jenkins DJ, Kendall CW, Augustin LS, Franceschi S, Hamidi M, Marchie A, and Axelsen M (2002). Glycemic index: Overview of implications in health and disease. The American Journal of Clinical Nutrition, 76(1): 266S-273S. https://doi.org/10.1093/ajcn/76.1.266S **PMid:12081850**

Jiang F, Du C, Jiang W, Wang L, and Du SK (2020). The preparation, formation, fermentability, and applications of resistant starch. International Journal of Biological Macromolecules, 150: 1155-1161. https://doi.org/10.1016/j.ijbiomac.2019.10.124 **PMid:31739041**

Kizil R, Irudayaraj J, and Seetharaman K (2002). Characterization of irradiated starches by using FT-Raman and FTIR spectroscopy. Journal of Agricultural and Food Chemistry, 50(14): 3912–3918. https://doi.org/10.1021/jf011652p **PMid:12083858**

Kusumayanti H, Handayani NA, and Santosa H (2015). Swelling power and water solubility of cassava and sweet potatoes flour. Procedia Environmental Sciences, 23: 164-167. https://doi.org/10.1016/j.proenv.2015.01.025

Lal MK, Singh B, Sharma S, Singh MP, and Kumar A (2021). Glycemic index of starchy crops and factors affecting its digestibility: A review. Trends in Food Science and Technology, 111: 741-755. https://doi.org/10.1016/j.tifs.2021.02.067

Leach HW (1959). Structure of starch granule I: Swelling and solubility patterns of various starches. Cereal Chemistry, 36: 534-544.

Liu JL, Tsai PC, and Lai LS (2021). Impacts of hydrothermal treatments on the morphology, structural characteristics, and in vitro digestibility of water caltrop starch. Molecules, 26(16): 4974. https://doi.org/10.3390/molecules26164974 **PMid:34443559 PMCid:PMC8401936**

Miller GL (1959). Use of dinitrosalicylic acid reagent for determination of reducing sugar. Analytical Chemistry, 31(3): 426-428. https://doi.org/10.1021/ac60147a030

Muhardina V, Lukmanul H, Patria A, Sulaiman I, and Zaidiyah Z (2016). Pasting properties, swelling and solubility of modified sweet potato starch of Acehnese local varieties using heat moisture treatment process. In the 2nd International Conference on Multidisciplinary Research University of Serambi Mekkah, Banda Aceh, Indonesia: 1–10.

Muir JG and O'Dea K (1992). Measurement of resistant starch: Factors affecting the amount of starch escaping digestion in vitro. The American Journal of Clinical Nutrition, 56(1): 123-127. https://doi.org/10.1093/ajcn/56.1.123 **PMid:1609748**

Nara S and Komiya TJSS (1983). Studies on the relationship between water-satured state and crystallinity by the diffraction method for moistened potato starch. Starch-Stärke, 35(12): 407-410. https://doi.org/10.1002/star.19830351202

Nassar NR, Heikal YA, Ramadan IE, and AM M (2017). Characteristics of pan bread and balady bread produced from different Saccharomyces cerevisiae strains. Egyptian Journal of Food Science, 45(1): 29-41.

Pons M and Fiszman SM (1996). Instrumental texture profile analysis with particular reference to gelled systems. Journal of Texture Studies, 27(6): 597-624. https://doi.org/10.1111/j.1745-4603.1996.tb00996.x

Pycia K, Gałkowska D, Juszczak L, Fortuna T, and Witczak T (2015). Physicochemical, thermal and rheological properties of starches isolated from malting barley varieties. Journal of Food Science and Technology, 52: 4797-4807. https://doi.org/10.1007/s13197-014-1531-3 **PMid:26243900 PMCid:PMC4519444**

Sasaki T and Matsuki J (1998). Effect of wheat starch structure on swelling power. Cereal Chemistry, 75(4): 525-529. https://doi.org/10.1094/CCHEM.1998.75.4.525

Singh J, Lelane C, Stewart RB, and Singh H (2010). Formation of starch spherulites: Role of amylose content and thermal events. Food Chemistry, 121(4): 980-989. https://doi.org/10.1016/j.foodchem.2010.01.032

Trinh KS and Dang TB (2019). Structural, physicochemical, and functional properties of electrolyzed cassava starch. International Journal of Food Science, 2019: 9290627. https://doi.org/10.1155/2019/9290627 **PMid:31192252 PMCid:PMC6525864**

Trinidad TP, Mallillin AC, Encabo RR, Sagum RS, Felix AD, and Juliano BO (2013). The effect of apparent amylose content and dietary fibre on the glycemic response of different varieties of cooked milled and brown rice. International Journal of Food Sciences and Nutrition, 64(1): 89-93. https://doi.org/10.3109/09637486.2012.700922 **PMid:22762237**

Wang S, Li C, Copeland L, Niu Q, and Wang S (2015). Starch retrogradation: A comprehensive review. Comprehensive Reviews in Food Science and Food Safety, 14(5): 568-585. https://doi.org/10.1111/1541-4337.12143

Wang W, Zhou H, Yang H, and Cui M (2016). Effects of salts on the freeze–thaw stability, gel strength and rheological properties of potato starch. Journal of Food Science and Technology, 53: 3624-3631. https://doi.org/10.1007/s13197-016-2350-5 **PMid:27777470 PMCid:PMC5069268**

Wiart C (2013). Medicinal plants of China, Korea, and Japan: Bioresources for tomorrow's drugs and cosmetics. Deutsche Zeitschrift für Akupunktur, 2(56): 56-57. https://doi.org/10.1016/j.dza.2013.06.029

Zhu T, Jackson DS, Wehling RL, and Geera B (2008). Comparison of amylose determination methods and the development of a dual wavelength iodine binding technique. Cereal Chemistry, 85(1): 51-58. https://doi.org/10.1094/CCHEM-85-1-0051